J Mol Model (2013) 19:559–569
DOI 10.1007/s00894-012-1578-x

ORIGINAL PAPER

Design of molecular switching and signaling based on proton transfer in 2-hydroxy Schiff bases: a computational study

Salem Abood Hameed · Saaban K. Alrouby · Rifaat Hilal

Received: 24 July 2012 / Accepted: 20 August 2012 / Published online: 9 September 2012

Abstract The present work aims to exploit the possibility of using the tautomerism in 2-hydroxy Schiff bases for molecular switching. The enol imine (E)⇔ enaminone (K) tautomerization in a series of 2-hydroxy Schiff bases have been investigated theoretically at the DFT/B3LYP/6-311G** level of theory. The intramolecular proton transfer processes have been explored, transition structures have been located and characterized. The kinetics and thermodynamics of the proton transfer process, and its time scale have been computed and discussed in the framework of the suitability as molecular switches. Substituent effects have been computed and its effect on the enthalpy changes (ΔH*) and activation energies (ΔG*) have been analyzed and discussed. Nonspecific solvent effects have also been taken into account by using the polarized continuum model (IPCM) of two different solvent. The tautomerization energies are decreased and hence the endothermic nature of the enol imine ⇔ enaminone tautomerization. The potential energy barriers, on the other hand, are increased due to the relative destabilization of the transition states. The NBO charge populations show that there is a high positive charge on the hydrogen atom during the process in all cases, which confirms that the proton transfer proceeds through a three-center interaction. The proton transfer processes, in all cases studied are kinetically allowed. The low potential energy barrier suggests that interconversion between the two tautomeric forms is spontaneous and the two forms may coexist.

Keywords DFT computation · Molecular switches · Proton transfer · Solvent and substituent effects · Tautomerism in Schiff bases

Introduction

Design and construction of devices is a major goal of science and technology. The top-down approach used so far for the construction of miniaturized devices is reaching fundamental and practical limits, which include severe cost limitations, for sizes below 50 nm.

Organic molecular materials are increasingly recognized as suitable molecular-level elements (such as switching, signaling, and memory elements [1, 2] for molecular devices, because the wide range of molecular characteristics can be combined with the versatility of synthetic chemistry to alter and optimize molecular structure in the direction of desired properties. True molecular switches undergo reversible structural changes, caused by a number of influences, which give a variety of possibilities for control. Several classes of photo responsive molecular switches are already known; these operate through processes such as bond formation and bond breaking, cis-trans isomerization, and photo induced electron transfer upon complexation [3].

The main requirement in the design of new molecular switches is to provide fast and clean interconversion between structurally different molecular states (on and off). Antonov et al. [4, 5] examined the possibility of using tautomerism for signaling and switching, because change in the tautomeric state can be accomplished by a fast proton transfer reaction between two or more structures, each of them with clear and different molecular properties [4, 5]. The present work continues on this line and aims to show how tautomerism can be exploited for signal conversion.

Electronic supplementary material The online version of this article (doi:10.1007/s00894-012-1578-x) contains supplementary material, which is available to authorized users.

S. Abood Hameed · S. K. Alrouby · R. Hilal (✉)
Chemistry Department, Faculty of Science, KAU,
Jeddah, Saudi Arabia
e-mail: rhilal@kau.edu.sa

2-hydroxy Schiff bases have been extensively studied [6–9]. This originated from the fact that the 2-hydroxy Schiff bases and their metal complexes exhibit wide applications, especially in biological systems [10–15]. The presence of ortho hydroxyl group in Schiff bases has been regarded as one of the important elements favoring for the existence of intramolecular hydrogen bonds and also the tautomerism accounting for the formation of either phenol-imine (O-H…N)(E-form) or keto-amine (O…H-N) (K-form) tautomers. A zwitterionic structure also appears due to a proton transfer in enol-imine and keto-amine tautomer. These classes of compounds also exhibit thermochromic and photochromic behavior (cf. scheme 1) [16].

Intramolecular hydrogen bonds and tautomerism between phenol-imine (E) and keto-amine (K) forms in 2-hydroxy Schiff bases in solution and in the solid state have been investigated by using different spectroscopic techniques [17–32]. However, the literature does not seem to arrive at a firm quantitative conclusion as to the relative stability and factors affecting the stability of these tautomeric forms.

It is the aim of the present work to exploit the possibility of using the tautomerism in 2-hydroxy Schiff bases for molecular switching. The intramolecular H-bond in a series of 2-hydroxy Schiff bases will be investigated at a high level of theory. The intramolecular proton transfer process will be explored; transition structures will be located and characterized. The kinetics and thermodynamics of the proton transfer process and its time scale will be computed and discussed in the framework of the suitability as molecular switches. Scheme 2 presents the 2-hydroxy Schiff bases studied in the present work.

Methods of calculations

All calculations have been carried out using the Gaussian09 [33] package of programs. The geometries of 2-hydroxy Schiff bases have been fully optimized at the DFT/B3LYP/6-311+G** level of theory [34–36]. Frequency calculations were performed at the same level of theory in order to characterize stationary points and to evaluate the zero-point energy (ZPE). Transition states were localized and identified. The IRC technique was used to construct the low energy reaction path for the proton transfer processes. The natural bonding orbitals (NBO) calculations [37] were performed using NBO 3.1 program as implemented in the Gaussian 09 package at the DFT/B3LYP/6-311+G** level in order to understand various second-order interactions between the filled orbitals of one subsystem and the vacant orbitals of another subsystem, which is a measure of the inter-molecular delocalization or conjugation, details are given elsewhere [38]. The solvent effect was studied using the isodensity polarizable continuum model (IPCM) [39] using the self-consistent reaction field (SCRF) method as implemented in the Gaussian 09 program which uses a static isodensity surface for the cavity and places the solute in a spherical cavity within the solvent reaction field. The solvents used were water and chloroform. In all tables and throughout the paper energy quantities are rounded to a four decimal places whereas, thermodynamics quantities are rounded to three decimal places only, just for the ease of presentation. Tables of higher accuracy (eight decimal places) of energy will be made available as a supplementary material.

Results and discussion

Figure 1 presents the optimized structure of the parent 2-hydroxy Schiff base studied in the present work. This structure is the global minimum on the potential energy surface. We have arrived at this global minimum in two steps. The first involved a full geometry optimization at the DFT/B3LYP/6-311G** level of theory. The geometry of the optimized structure is used as a starting input for a molecular dynamics computation. A search in the three dimensional conformational space has been performed. The planarity of the composite molecule is governed mainly by three torsion angles, namely the two dihedral angles governing the co-planarity of the two phenyl rings and the dihedral angle governing the orientation of the OH group.

In the global minimum structure the OH group is pointing toward the C = N group suggesting the possibility of H-bonding. This point has been explored by computing the potential energy profile of rotation around the ph-OH torsion angle. The computed H-bond energy is -16.2375 kcalmol^{-1} at a H-bond length = 1.7329 A°. Thus, at a typical H-bond length, the energy is considerably large confirming a major role for this H-bond in stabilizing the global minimum structure and a possible major role in the proton transfer process.

It is interesting to analyze the charge density distribution in the OH and C = N bond regions. The ph-O bond length is considerably shorter than a typical C-O bond. The OH bond

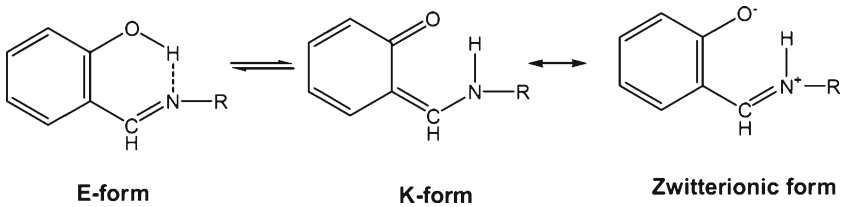

Scheme 1 The three possible tautomeric forms of 2-hydroxy Schiff bases

Scheme 2 2-hydroxy Schiff bases studied in the present work and the numbering system adopted

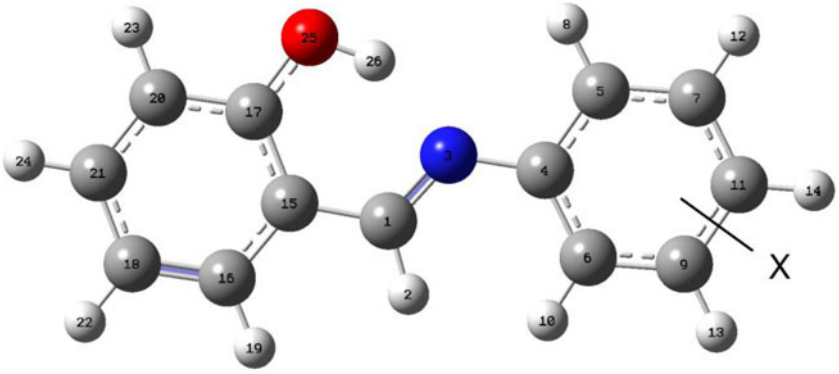

X=H (1) p-NO2 (2) ; o-NO2(3);p-oCH3(4); o-Cl (5)

is highly polarized, with a net negative charge of 0.343 e on the O atom. This marked ionic character of the OH bond, facilitates the possibility of proton transfer to the negative nitrogen atom. Table 2 presents some geometric parameters in the enol imine conformation of 1.

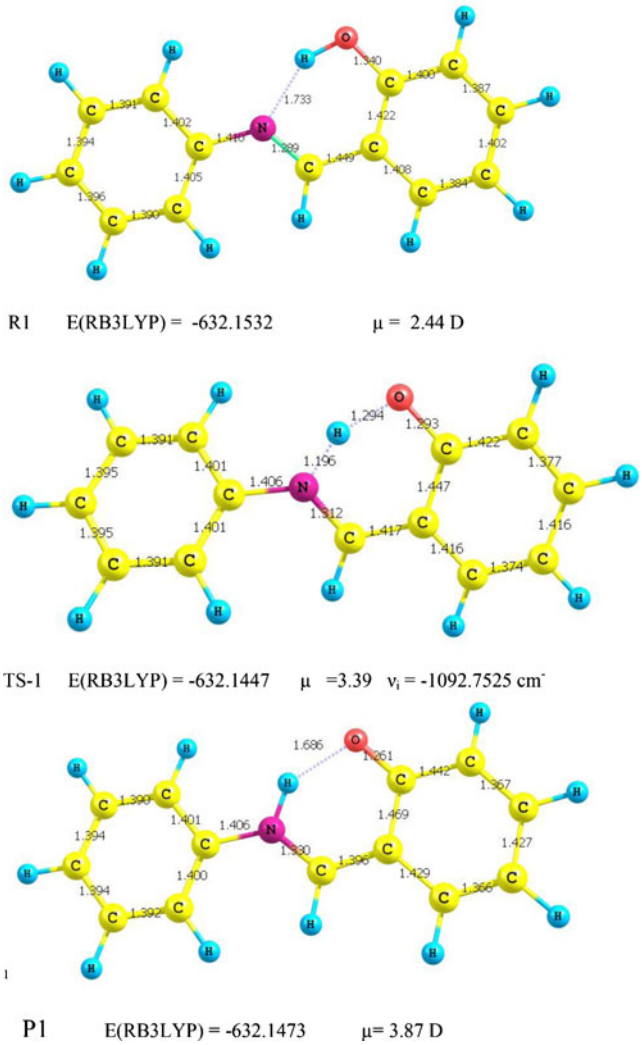

Fig. 1 Fully optimized geometric structures and charge densities of the enol-imine, keto-amine and the transition state of the proton transfer process for **1**

Natural bond order

Natural bond order analysis indicates that resonance permits strongly delocalized structure. Thus, the total Lewis contribution is dominating. Table 1 presents second order perturbation theory analysis of Fock matrix in NBO basis for the parent Schiff base 1. The values selected in this table represent major donor-acceptor interactions between natural orbitals whose interaction energies are greater than 10 kcal mol^{-1}. In the following discussion we will focus on the interactions involving the C = N and the OH groups with the rest of the molecule. The C = N bond is typical double bond, interacting strongly with the π-system via the C4-C5 and the C15-C17 antibonding orbital. The C = N group acts as both donor and acceptor in these interactions. The interaction with the π-systems of the two phenyl rings indicates the linear conjugation in this molecule. The interactions among the virtual orbitals are, however, more pronounced. On the other hand, the most dominant interaction involving the hydroxyl group oxygen atom is the lone pair interaction with the π system (37.10 kcal mol^{-1}).

One should note first that for the parent compound 1, the keto structure maintain the co-planarity of the molecule. The CN bond length is stretched from a value of 1.289 Å to 1.330 where the CO bond is reduced to a value of 1.261 Å. The Ph-CN bond length is much shorter than a typical C-C bond length indicating a considerable π-bond character in this region. The enol-keto tautomerism is characterized by a considerable increase in the dipole moment from a value of 2.44 D to 3.87 D. This property may very well underlie the use of this tautomeric equilibrium for creating a molecular switching and signaling.

The donor-acceptor interactions in the K-form of compound 1 is different from that discussed before for the corresponding E-form. Thus, in the K-form the cross conjugation prevails

Table 1 Second order perturbation theory analysis of Fock matrix in NBO basis for the parent Schiff base 1

Donor NBO(i)	Acceptor NBO(j)	E(2), Kcal/mol	E(j)-E(i) Kcal/mol	F(i,j), a.u
E-form				
BD(2)C1-N3	BD*(2)C4-C5	13.68	0.36	0.068
BD(2)C4-C5	BD*(2)C1-N3	15.15	0.26	0.058
BD(2)C4-C5	BD*(2)C6-C9	19.30	0.28	0.066
BD(2)C4-C5	BD*(2)C7-C11	20.65	0.28	0.69
BD(2)C6-C9	BD*(2)C4-C5	19.92	0.29	0.068
BD(2)C6-C9	BD*(2)C7-C11	18.83	0.29	0.066
BD(2)C7-C11	BD*(2)C4-C5	20.43	0.28	0.068
BD(2)C7-C11	BD*(2)C6-C9	20.81	0.28	0.068
BD(2)C15-C17	BD*(2)C1-N3	22.61	0.26	0.072
LP(1)N 3	BD*(1)C1-H2	11.62	0.74	0.085
LP(2)O25	BD*(2)C15-C17	37.10	0.33	0.105
BD*(2)C1-N3	BD*(2)C4-C5	47.59	0.02	0.056
BD*(2)C1-N3	BD*(2)C15-C17	136.02	0.02	0.073
K-form				
BD(2)C1-C15	BD*(2)N3-C 4	9.03	0.21	0.044
BD(2)C1-C15	BD*(2)C17-O25	28.30	0.28	0.080
BD(2)N3-C4	BD*(2)C1-C15	35.83	0.34	0.100
BD(2)C5-C7	BD*(2)N3-C4	32.43	0.21	0.084
BD(2)C6-C 9	BD*(2)N3-C4	33.67	0.21	0.087
BD(2)C20-C21	BD*(2)C17-O25	26.29	0.27	0.079
LP (1) O25	RY*(1) C17	11.38	1.56	0.119
LP (1) O25	BD*(1)N3-H26	6.29	1.04	0.073
LP (2) O25	BD*(1)N3-H26	26.46	0.70	0.123
LP (2) O25	BD*(1)C15-C17	11.13	0.77	0.084
LP (2) O25	BD*(1)C17-C20	16.09	0.80	0.104
BD*(2)C1-C15	BD*(2)C16-C18	45.04	0.03	0.064
BD*(2)N3-C4	BD*(2)C1-C15	41.40	0.06	0.059
BD*(2)N3-C4	BD*(2)C5-C7	80.23	0.08	0.093
BD*(2)N3-C4	BD*(2)C6-C9	89.19	0.07	0.095
BD*(2)C17-C25	BD*(2)C20-C21	80.07	0.03	0.081

where the nitrogen atom enjoys interaction with the π-system of th N-Ph ring mainly. The oxygen lone pair interacts with the carbon Rydberg orbitals and the antibonding N-H orbital. The keto-enol tautomerization process is accompanied by a major redistribution of the charge density. Thus, the carbonyl oxygen atom behaves as an electron sink localizing≈0.4 e while the imino-nitrogen atom is only slightly negative.

NBO analysis of the K-form show that C4 and C15 are of notably low occupancies and there exist a major interaction between the C-N bonding MO with Rydberg orbitals of C4 and C15 amounts of 2.56 and 2.29 kcalmol^{-1}, respectively. The localized benzonoid nature of the N-phenyl ring is evident from a high interaction energy between the N-C and the phenyl C-C anti-bonding orbitals that amounts to 35.98 kcal mol^{-1} for the N-C4, C1-C15 interaction. On the other hand, in the quinonoid ring the interaction of C = O group with the rest of the composite system is rather weak, indicating cross-conjugation in this region. The population of the valence lone pair orbital of the oxygen atom is relatively low, 1.861.

In contrast to the case of the E-form, the HOMO of the K-form is almost localized completely on the N-ph moiety (cf. Fig. 2).

The Zwitterionic structure of the parent Schiff base 1 is rather much less stable than the enol-form, thus the change in the heat of formation for the enol⇔ zwitterion is $\Delta H^{\#}$= 280.3942 kcalmol^{-1}. The reaction keto⇔ zwitterion is also endothermic with a heat of formation of 276.7971 kcal mol^{-1}. Therefore, the existence of the zwitterion species is irrelevant to our discussion and will therefore be omitted.

The transition state

The transition state for the proton transfer reaction has been localized and identified in three main computational steps.

Table 2 Some selected geometric structural parameters in the proton transfer region (bond length in Å; angles in degrees all energy quantities are in Hartree)

Parameter	Keto-amine form(P)	Transition state(TS)	Enol-imine form(R)
C-O	1.262	1.293	1.340
O-H	1.685	1.294	0.993
N-H	1.044	1.196	1.793
N-C	1.332	1.312	1.289
N-C(ph)	1.395	1.406	1.410
NC-C	1.405	1.417	1.448
C-C(ph)[a]	1.427–1.366	1.420–1.377	1.408
C-C(ph)[b]	1.394	1.392	1.402
OHN	140.8	147.9	152.5
CCC	120.0	118.9	121.6
CCN	122.6	119.6	122.2
CNC(ph)	128.4	126.1	123.5
E	−631.9297	−631.9305	−631.9356
H	−631.9288	−631.9296	−631.9346
G	−631.9779	−631.9804	−631.9836
ZPE	0.2067	0.2028	0.2067

E total energy *H* standard enthalpy *G* standard free energy
ZPE zero point energy
[a]C-C bond length in hydroxyphenyl ring
[b]C-C bond length in the N-Ph ring.

The first involves locating the high energy structure involving the transfer of the proton from the oxygen to the nitrogen center. One straightforward way to estimate the transition-state structure is to perform a scan of the potential energy surface describing the migration of the hydrogen atom. This can be readily accomplished in a calculation that utilizes internal, rather than Cartesian coordinates. Using this approach, the O…H…N bond angle can be systematically varied, allowing the H atom to pass through the transition-state area. The obtained partially optimized structure is now used as input for a transition state and frequency computation to obtain the structure of the transition state. This fully optimized structure is presented in Fig. 3.

The transition state is characterized by one and only one negative vibrational frequency (shown in Fig. 3 in light blue). This represents the reaction coordinate and involves only the O….H…..N vibrations. The magnitude of the imaginary frequency (1092 cm^{-1}) indicates a marked curvature of the potential energy profile. The transition state is more polar than the starting E-structure, thus is more stabilized in polar solvent. Furthermore, the transition structure is characterized not only by a greater dipole moment, but also a change in its direction; a point of prime importance in the context of our investigation in this paper.

The transition state shows accumulation of (−0.45 e) charge density on the oxygen atom. The nitrogen atom on the other hand, approaches an sp3 hybridization carrying a partially positive charge of 0.393 e. The hydrogen atom, in the transition state is closer to the nitrogen atom with the subsequent shortening of the C-O bond length approaching its value in the keto-amine form. The transition state structure falls closer to a great extent to that of the product. Some selected geometric parameters of the starting, transition state and final structures are presented in Table 2 and in Fig. 2.

At this point, with the transition state located and characterized, one moves to the third and final step in its characterization, namely, to perform intrinsic reaction coordinate (IRC) calculations of the proton transfer process. The IRC potential, represents here the minimum energy pathway (MEP) that connects a transition state with a stable entity. The “forward” and “reverse” directions along the IRC potential lead either to enol-imine or keto-amine tautomers depending on the nature of the algorithm. The IRC, moreover, accounts quantitatively for the displacement of all atoms along this path. The IRC calculation produces the energy profile presented in Fig. 4. It should also be noted that, in the transition state, the structure is almost already relaxed from the benzonoid to the quinonoid geometry.

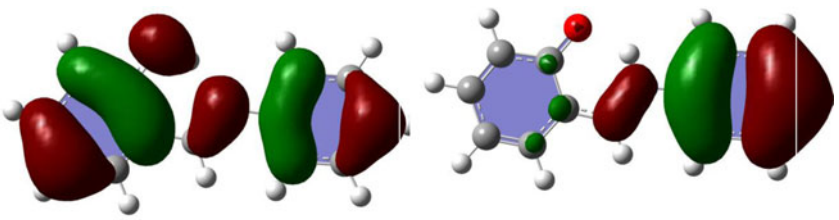

Fig. 2 Charge density distributions of the HOMO’s for the E- and the K-forms of **1**

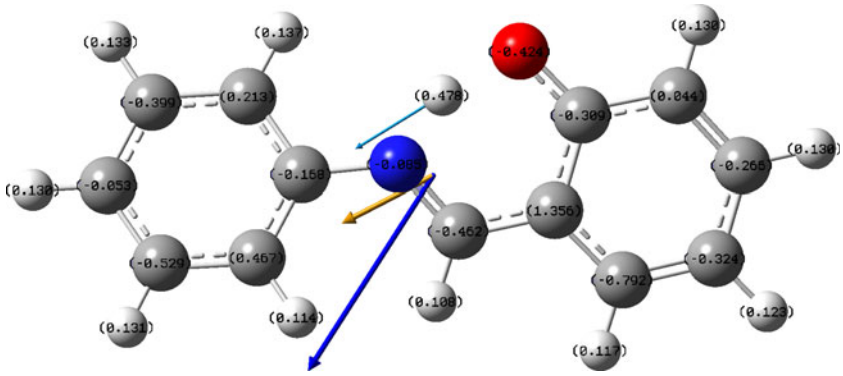

Fig. 3 Fully optimized structure of the transition state for the proton transfer process for **1**. The vibration vector (reaction coordinate) is shown in *light blue*, the dipole displacement vector in *yellow* and the dipole moment vector in *deep blue*

Energy considerations

Let us examine the energetic of the proton transfer process. Figure 4 presents the potential energy profile for the keto-enol tautomerization. The enol-imine form is more stable by 3.699 kcal mol^{-1} indicating the endothermic nature of the tautomerization process. The barrier height for the transformation is 5.350 kcal mol^{-1} for the forward reaction and is much lower (1.649 kcal mol^{-1}) for the backward reaction. It should be noted that the values of $\Delta H^{\#}$ and $\Delta G^{\#}$ are so small that it is less than the thermal energy at room temperature.

With the information obtained it is possible to estimate the reaction enthalpies, equilibrium constants, and the rate constants for these processes. Table 3 lists the reaction enthalpies and equilibrium constants. To obtain the rate constants, we will first apply the RRK theory [38], assuming that energy is randomly distributed among the vibrational degrees of freedom. Using the expression for the high-

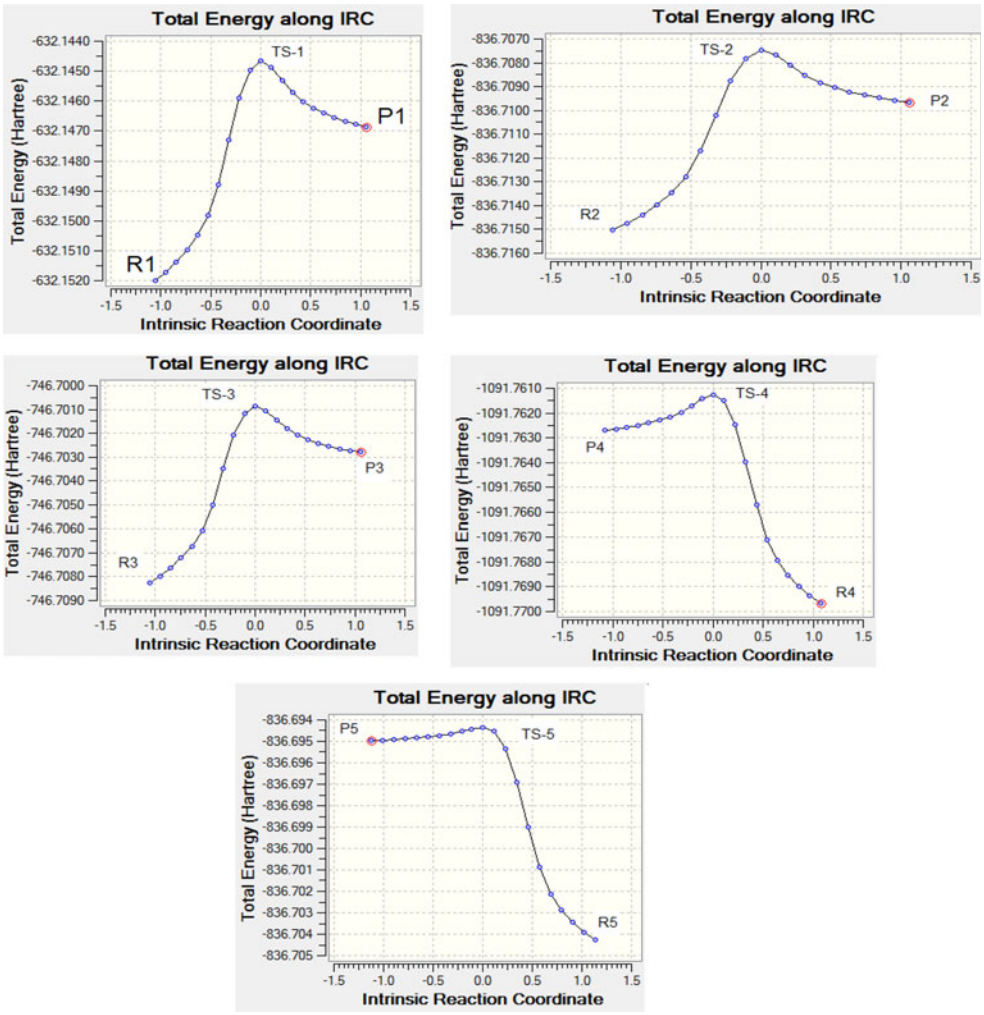

Fig. 4 IRC for the proton transfer reactions of the studied Schiff bases

Table 3 Summary of Thermodynamics and kinetic properties of enol-imine-keto-enamine tautomerism for the 2-hydroxy Schiff bases studied in the present work

Property	1	2	3	4	5
$\Delta H^{\#}$	−3.699	−5.176	−4.811	−5.969	−7.809
$\Delta G^{\#}$(f)	−5.350	−6.912	−6.758	−6.749	−8.285
$\Delta G^{\#}$(b)	−1.649	−1.732	−1.396	−0.782	−0.475
K^o	1.944×10^{-3}	1.604×10^{-4}	1.5476×10^{-4}	4.2509×10^{-5}	1.8987×10^{-6}
K_{TST}/s^{-1} forward	7.488×10^{8}	5.3721×10^{7}	5.9033×10^{7}	7.0729×10^{7}	5.300×10^{6}
	9.3×10^{-8}	1.17×10^{-8}	1.6849×10^{-8}	8.878×10^{-12}	1.1867×10^{-11}
K_{TST}/s^{-1} backward	3.8526×10^{11}	3.3493×10^{11}	3.8145×10^{11}	1.663×10^{12}	2.7913×10^{12}
	1.632×10^{-12}	1.878×10^{-12}	1.0655×10^{-12}	3.782×10^{-11}	2.253×10^{-11}
v_i/cm^{-1}	1092.75i	1098.38i	1066.61i	982.70i	762.23i

$\Delta H^{\#}$ Standard enthalpy change for enol⇔ keto tautomerization reaction

$\Delta G^{\#}$ (f) change in the standard free energy for the forward R1 to TS-1 reaction

$\Delta G^{\#}$ (b) change in the standard free energy for the backward P1 to TS-1 reaction

K^o equilibrium constant k(forward)/k(backward)

K_{TST}/s^{-1} forward rate constant for the forward reaction

K_{TST}/s^{-1} backward rate constant for the backward reaction

pressure limit [40]:

$$k_{RRK} = -\nu_i \exp\left(-E_o/k_B T\right) \quad (1)$$

where ν_i is the frequency (in Hz) of the critical oscillator (i.e., the magnitude of the imaginary frequency) and E_0 is the difference in zero-point energies of the transition state and reactant. One can also estimate the rate constant from transition state theory (TST) formulation [41] using:

$$k_{TST} = k_B T/h \exp\left(-\Delta G^{\#}/RT\right) \quad (2)$$

where k_B and h are Boltzmann's and Planck's constants, respectively, $\Delta G^{\#}$ is the change in the standard Gibbs free energy between the transition state and enol-imine species (including the respective zero-point energies) values obtained are in close agreement with the RRK results. Results of our calculations are presented as k_{TST} in Table 3. One can readily conclude that both tautomeric forms are kinetically stable species at ambient temperatures, although the keto-amine form is thermo-dynamically unstable with respect to the unimolecular tautomerization process.

Effect of substitution

Geometry considerations

The main requirement in the design of new molecular switches is to provide fast and clean interconversion between structurally different molecular states, in our case, tautomeric forms (on and off). The sensitivity of the electronic ground and excited states of the tautomeric forms to environment stimuli (light, pH value, temperature, solvent) and to the presence of a variety of substituents can be exploited in the design of flexible tools for control. In the present section, the effect of substituents of different electron accepting/donating tendency will be explored. The effect of solvents of different dielectric constants will be investigated and discussed in the next section.

The first substituent that will be investigated is the strong electron withdrawing nitro group. This group has a pronounced perturbing effect and thus one would expect a marked change in geometry and charge density distributions. The optimized geometric structure of the p-nitro derivative of the enol-imine tautomer is shown in Fig. 5a. The molecule is not co-planar with the nitrophenyl moiety out of the plane of the rest of the molecule by 40°. This molecule is not only characterized by large dipole moment (μ=6.04 D) but also with a drastic change in its direction. The NO_2-group acts as an electron sink accumulating 0.25e on the expense of the phenyl ring. The nitrogen atom of the C = N is slightly positive, whereas the O-H bond shows strong ionic character.

Figure 5a, 5b presents the keto-amine form of the p-nitro derivative. The molecule is coplanar with a slightly reduced dipole moment. The corresponding transition state is presented in Fig. 5a. The transition state structure is approaching coplanarity (out-of plane angle is 18°) with an appreciable dipole moment of 5.55 D pointing in almost the same direction as that in the enol imine tautomer. The presence of the NO2-group in the ortho position causes a marked steric hindrance which forces the NO_2Ph moiety out of the plane of the molecule by 83°. The dipole moment is reduced to 4.54 D.

p-Methoxy substitution causes the methoxyphenyl moiety to be out of plane by 30°. The dipole moment is considerably reduced to a value of 2.35 D. The charge density

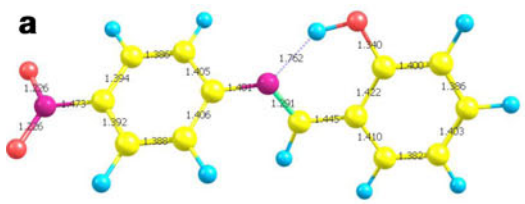

E= -836.7185 μ= 6.042 D

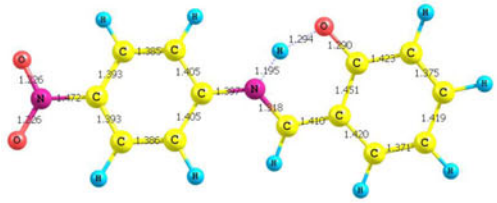

E= -836.7075 ν_i =1098.38 cm^{-1}

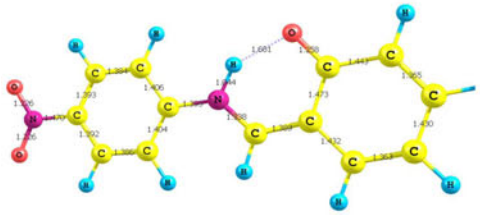

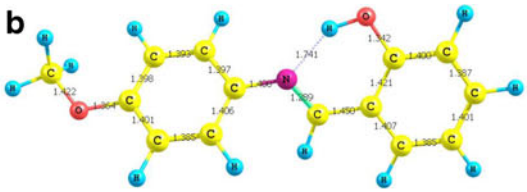

E= -746.7107 μ=2.35 D

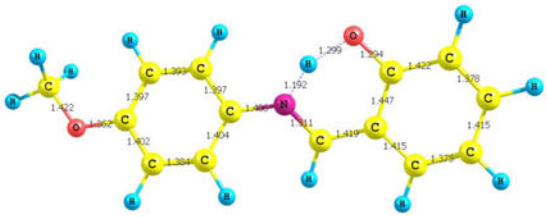

E=-746.7008 ν_i=1066.5cm^{-1}

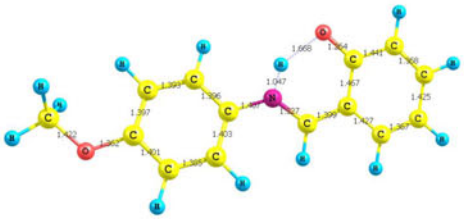

E= -746.7031 μ. =3.77 D

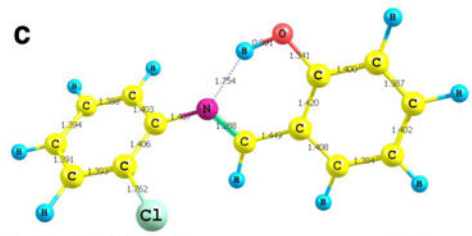

E= -E=- 1091.7725 H. μ= 2.23 D

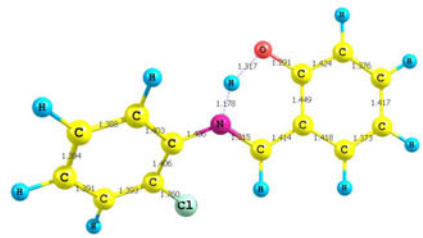

E= -1091.7613 ν_i =-982.71cm^{-1}

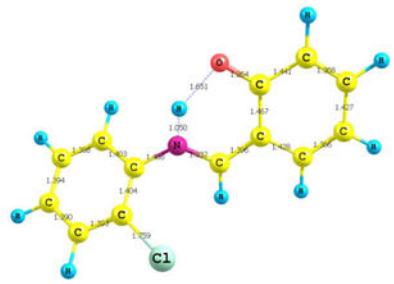

E=-1091.7630 μ. = 3.77 D

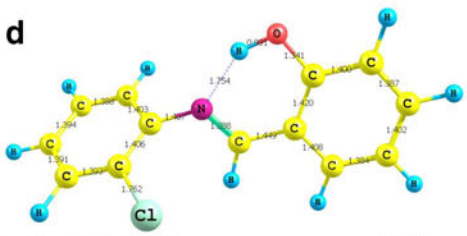

E= -E=- 1091.7725 H. μ= 2.23 D

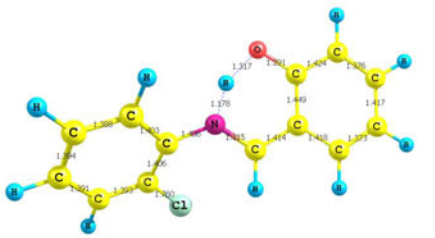

E= -1091.7613 ν_i =-982.71cm^{-1}

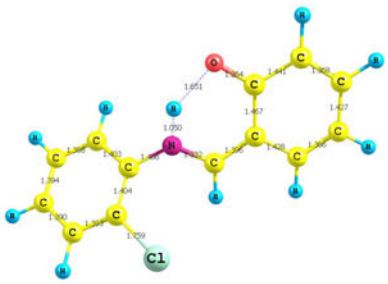

E=-1091.7630 μ. = 3.77 D

◀ **Fig. 5** Optimized structures of the enol, keto- and transition states for the substituted Schiff Bases studied in the present work **a** P-NO2, **b** p-OCH3, **c** o-OCH3 **d** o-Cl

distribution is rather different, thus the imine nitrogen atom carries −0.554 e whereas, the OH is more polar with the oxygen atom and acts as electron sink that accumulates 0.6990 e. The keto amine tautomeric form suffers an increase in the magnitude of the dipole moment and inflection of its direction. The structure is approaching co-planarity with an out of plane angle of 14°. The corresponding transition state resembles to a great extent the keto-amine tautomer.

Although, o-Chloro substitution does not introduce any new geometrical features, it still forces the molecule to be non co-planar with an out of plane angle of 60°. The dipole moment is reduced and pointing toward the chloro substituent. Figures 4 and 5 summaries the geometric and dipolar properties of the Schiff bases studied.

Natural bond order analysis

NBO charge distribution was also analyzed according to the results calculated at the B3LYP/6-311G** level. For analyzing these results, it would be useful to follow the evolution of charge separation along the reaction path. We have considered the charge on labile hydrogen H26, O25 and N3 and so on. The Mulliken and NBO charge populations show that there is a high positive charge on the hydrogen atom during the process in all cases, which confirms that the reaction corresponds to a proton transfer. Furthermore, the proton transfer proceeds through a three-center interaction. As a typical behavior of a proton transfer process, the net charge of the donor oxygen atom increases; whereas that of the acceptor nitrogen decreases. The population of charge for the donor oxygen is much larger than that of the acceptor nitrogen. So, there is a π-electronic transfer from the donor oxygen to the acceptor nitrogen through the conjugated π-system. The charge on labile hydrogen H1 decreases during the process of intramolecular proton transfer and its positive charge becomes more positive in the enol-imine forms.

Solvent effect

To extend our understanding of the enol imine ⇔ enaminone tautomerization, we have examined the effect of solvent polarity on the potential energy surface for the tautomerization process. The standard approach of the IPCM (without any explicit solvent molecules), as it is used here, appears to be a good first step in the theoretical investigation of the effect of solvent on tautomeric equilibrium of Schiff bases.

The energy of each tautomer in the presence of a continuous solvent dielectric was explored to determine the effects of a solvents dielectric on the tautomer energy differences. All the species were stabilized by the dielectric constant of the solvent. Table 4 presents the solvation energies and activation energies (the free energy change) for the tautomerization reaction ΔG#. Careful inspection of the data presented in this table reveals that the keto amine form is stabilized by polar solvent to a much greater extent than the enol form and the transition structure. This is due to the higher polarity of the keto form and the fact that it is much more polarized. The effect of this solvation is the decrease of the endothermic nature of the tautomerization reaction. This is true for all Schiff bases studied. Energy quantities presented in Table 3 indicate that the enol form is more stable than the keto form in the gas phase, in polar and non-

Table 4 Solvation energies ($kcal\,mol^{-1}$) and activation energies (free energy changes $\Delta G^{\#}$) for the tautomerization reaction of Schiff bases studied in the present work computed at the B3LYP/6-311G** level using the isodensity polarizable continuum solvent model

Compounds	$\Delta G^{\#}$ (gas phase)	Solvation energy, kcal/mol		$\Delta G^{\#}$ in solution	
		Water	Chloroform	Water	Chloroform
R1		−9.354	−7.100		
TS-1	5.350//−1.649−	−6.505	−4.975	8.198//−8.04−	*
P1		−12.897	−9.647		
R2		−8.050	−6.186		
TS-2	6.912//−1.732−	−9.770	−7.470	−5.191//−2.730	−5.627/−/2.476
P2		−10.768	−8.214		
R3		−9.983	−7.566		
Ts-3	−6.758//−1.396	−7.888	−6.050	−8.305//−2.444	−7.726//−2.178
P3		−8.935	−6.832		
R4		−8.928	−6.829		
TS-4	−6.749/−0.782	−5.862	−4.431	−9.818//−6.962	−9.152//−5.404
P4		−12.042	−9.053		
R5		−7.458	−5.742		
TS-5	−8.289/−/0.475	−8.971	−6.886	6.775//−1.066−	−7.145//−1.315

$\Delta G^{\#}$ standard free energy change are given for forward/backward reactions

* Calculation of the TS failed to converge

polar solvents. This is in agreement with previous experimental studies on Schiff bases. The UV-visible spectra of some 2-hydroxy Schiff bases were also studied in polar and non-polar solvents [42–44]. For the Schiff bases derived from salicylaldehyde and aniline, the ketoenamine form was not observed in polar and non-polar solvents, but was noted after acid addition. Such a difference could be caused by the loss of aromaticity in going from E to K form in compound 1, the number of delocalized electrons in the tautomeric phenyl ring is reduced from six to four in going to the K form because two of those electrons are engaged in the strong C = N and C = O bonds. Thus, the phenyl ring loses much of its aromaticity. Both polar and non-polar solvents lift the potential energy barrier. This is due to the fact that, transition states are less polar than both of the tautomeric forms and hence are much less stabilized by solvents.

Conclusions

Table 3 summarizes the thermodynamics and kinetic properties of the studied Schiff bases. In all cases, the energy barriers are small amounts to a maximum value of 8.8 kcal mol^{-1} in the forward direction. Furthermore, the barrier height in the backward direction is much less and reaches a minimum value of 0.47 kcalmol^{-1}. This is less than the thermal energy (3/2 kT) at room temperature. Thus, the proton transfer processes, in all cases studied are kinetically allowed. The low potential energy barrier suggests that interconversion between the two tautomeric forms is spontaneous and the two forms may coexist. This is further supported by the work of Makenzie et al. that quantum tunneling below the energy barrier associated with the transition state, significantly enhances the reaction rate in many proton transfer reactions [45].

Results of the present work show that substitution would have a significant impact on the potential energy barrier for the proton transfer process. The keto-amine form seems to be much more affected by substitution than the corresponding enol-imine form. The electron withdrawing groups studied, NO_2 and Cl, especially when substituted in the o-position have the effect of considerably lowering the barrier, to reach the value of 0.8 and 0.5 kcalmol^{-1}, respectively. This barrier is much less than the thermal energy at room temperature suggesting a spontaneous interconversion between the two tautomeric forms. One therefore may conclude that development of molecular switching and signaling device based on this tautomerism is feasible where on/off signaling can be achieved by changing solvent dielectric constant.

Proton potential functions, in agreement with our expectations, suggest that there is no minimum at the acceptor side, but the energy necessary to move the proton is not large, so it is possible for the proton to move into the acceptor region. This fact enabled us to proceed further with the structural analyses on the basis of geometric and electronic structure parameters. It should also be noted that, proton transfer from the imino enol tautomer to the keto amine form is accompanied by a benzenoid-quinonoid structural change with a concomitant loss of aromaticity. Although the studied Schiff bases show much higher stability for azo (imino enol) tautomers, there is an appreciable quinone content in the studied Schiff bases. This content increases with the electron accepting power of the substituent.

References

1. Balzani V, Piotrowiak P, Rodgers MAJ, Mattay J, Astruc D, Gray HB, Winkler J, Fukuzumi S, Mallouk TE, Hass Y, de Silva AP, Gould I (2001) Electron transfer in chemistry, vol 1. Wiley-VCH, Weinheim
2. Feringa BL (2001) Molecular switches, vol 1. Wiley-VCH, Weinheim
3. Andreasson J, Straight SD, Moore TA, Moore AL, Gust D (2008) J Am Chem Soc 130:11122–11128
4. Antonov L, Deneva V, Simeonov S, Kurteva V, Nedeltcheva D, Wirz J (2009) Exploiting tautomerism for switching and signaling. Angew Chem Int Ed 48:7875–7878
5. Hynes JT, Klinman JP, Limbach HH, Schowen RL (2007) Hydrogen-transfer reactions, vol 1. Wiley-VCH, Weinheim
6. Filarowski A, Koll A, Sobczyk L (2009) Curr Org Chem 13:172–193, and references cited herein
7. Nedeltcheva D, Antonov L, Lycka A, Damyanova B, Popov S (2009) Curr Org Chem 13:217–239, and references cited herein
8. Sheikhshoaie I, Fabian WMF (2009) Curr Org Chem 13:149–171, and references cited herein
9. Krygowski TM, Wozniak K, Anulewicz R, Pawlak D, Kolodziejski W, Grech E, Szady A (1997) J Phys Chem 101:9399–9404
10. Filarowski A, Koll A, Głowiak T, Majewski E, Dziembowska T (1998) Ber Bunsenges Phys Chem 102:393–402
11. Filarowski A, Koll A, Głowiak T (2002) J Mol Struct 615:97–108
12. Filarowski A, Kochel A, Cieślik K, Koll A (2005) J Phys Org Chem 18:986–993
13. Raczynska ED, Krygowski TM, Zachara JE, Osmialowski B, Gawinecki R (2005) J Phys Org Chem 18:892–897
14. Grabowski SJ, Sokalski WA, Leszczynski J (2006) J Phys Chem A 110:4772–4779
15. Grabowski SJ, Sokalski WA, Dyguta E, Leszczynski J (2006) J Phys Chem B 110:6444–6446
16. Palusiak M, Simon S, Sola M (2006) J Org Chem 110:5875–5822
17. Palusiak M, Krygowski TM (2007) Chem Eur Chem 13:7996–8006
18. Zubatyuk RI, Volovenko YM, Shishkin OV, Gorb L, Leszczynski J (2007) J Org Chem 72:725–735
19. Filarowski A, Kochel A, Kluba M, Kamounah F (2008) J Phys Org Chem 21:939–944
20. Kluba M, Lipkowski P, Filarowski A (2008) Chem Phys Lett 463:426–430
21. Karabiyik H, Petek H, Iskeleli NO, Albayrak C (2009) Struct Chem 20:903–910
22. Karabiyik H, Petek H, Iskeleli NO, Albayrak C (2009) Struct Chem 20:1055–1065
23. Martyniak A, Lipkowski P, Boens N, Filarowski A (2012) J Mol Model 18:257–263

24. Filarowski A, Koll A, Gzowiak T (2002) J Chem Soc Perkin Trans 2:835–842
25. Rospenk M, Król-Starzomska I, Filarowski A, Koll A (2003) Chem Phys 287:113–124
26. Harzfeld R, Nagy P (2001) Curr Org Chem 5:373–394
27. Dudek GO, Dudek EP (1966) J Am Chem Soc 88:2407–2412
28. Dziembowska T, Rozwadowski Z, Filarowski A, Hansen PE (2001) Magn Reson Chem 39:67–87
29. Salman SR, Saleh NAI (1997) Spectr Lett 30:1289–1300
30. Kownacki K, Mordzinski A, Wilbrandt R, Grabowska A (1994) Chem Phys Lett 227:270–276
31. Grabowska A, Kownacki K, Kaczmarek L (1994) J Lumin 1:886–890
32. Ogawa K, Harada J, Fujiwara T, Yoshida S (2001) J Phys Chem A 105:3425–3427
33. Frisch MJ et al (2003) Gaussian 09. Gaussian Inc, Pittsburgh PA
34. Becke AD (1993) J Chem Phys 98:5648–5652
35. Becke AD (1993) J Chem Phys 98:1372–1377
36. Lee C, Yang W, Parr RG (1988) Phys Rev B 37:785–789
37. Glendening ED, Reed AE, Carpenter JE, Weinhold F (2003) NBO Version 3.1, GaussianInc, Pittsburg
38. Reed AE, Curtiss A, Weinhold F (1988) Chem Rev 88:899–926
39. Barone V, Cossi M, Tomasi J (1989) J Comput Chem 19:404
40. Baghal-Vayjooee MH, Callister MH, Prichard HO (1977) Can J Chem 55:2634–1636
41. Steinfeld JI, Francisco JS, Hase WL (1989) Chemical kinetics and dynamics, 2nd edn. Prentice Hall, Upper Saddle River, pp 300–301
42. Ogawa K, Harada J, Fujiwara T, Yoshida S (2001) J Phys Chem A105:3425–3427
43. Ledesma G, Ibanez G, Escandar G, Olivieri AC (1997) J Mol Struct 415:115–121
44. Salman SR, Shawkat SH, Al-Obaidi GM (1990) Can J Spectrosc 35:25–27
45. Bothma JP, Gilmore J, Mckenzie RH (2010) New J Phys 12:055002